



# Thermal conductivity prediction of nanofluids containing CuO nanoparticles by using correlation and artificial neural network

Ali Komeilbirjandi<sup>1</sup> · Amir Hossein Raffiee<sup>2</sup> · Akbar Maleki<sup>3</sup> · Mohammad Alhuyi Nazari<sup>4</sup> · Mostafa Safdari Shadloo<sup>5</sup>

Received: 18 July 2019 / Accepted: 13 September 2019 / Published online: 23 September 2019  
© Akadémiai Kiadó, Budapest, Hungary 2019

## Abstract

Nanofluids are employed in different thermal devices due to their enhanced thermophysical features which lead to noticeable heat transfer augmentation. One of the major reasons of the heat transfer improvement by using the nanofluids is their increased thermal conductivity. Several methods have been applied to estimate this property of nanofluids such as correlations and artificial neural networks (ANNs). In the present paper, group method of data handling (GMDH) and a mathematical correlation are proposed for forecasting the thermal conductivity of nanofluids containing CuO nanoparticles. The inputs of the both models are the base fluids' thermal conductivities, concentration, temperature and nanoparticle dimension. Comparison of the forecasted data by these two approaches revealed more favorable performance of GMDH. The values of *R*-squared in the cases where polynomial and ANN were utilized were 0.9862 and 0.9996, respectively. Moreover, the average absolute relative deviation values were 5.25% and 0.881% for the indicated methods, respectively. According to these statistical values, it is concluded that employing the ANN-based regression leads to more confident model for forecasting the TC of the nanofluids containing CuO nanoparticles.

**Keywords** Nanofluid · GMDH · Thermal conductivity · Artificial neural network

## List of symbols

$a_i$	<i>i</i> th coefficient
$x$	Input vector
$x_1$	Temperature of nanofluid (°C)
$x_2$	Volume fraction of solid phase (%)
$x_3$	Size of particles (nm)
$x_4$	Thermal conductivity of the base fluid ( $\text{W m}^{-1} \text{K}^{-1}$ )
$y$	Output vector

$y_i^{\text{experimental}}$	Measured data in experiment
$y_i^{\text{predicted}}$	Predicted value by the model

## Abbreviations

AARD	Average absolute relative deviation
ANN	Artificial neural network
GMDH	Group method of data handling
MSE	Mean square error
RD	Relative deviation

✉ Akbar Maleki  
akbar.maleki20@yahoo.com; a\_maleki@shahroodut.ac.ir;  
a\_maleki@ut.ac.ir

<sup>1</sup> Department of Civil, Geo and Environmental Engineering, Technical University of Munich, Munich, Germany

<sup>2</sup> School of Mechanical Engineering, Purdue University, West Lafayette, IN, USA

<sup>3</sup> Faculty of Mechanical Engineering, Shahrood University of Technology, Shahrood, Iran

<sup>4</sup> Department of Renewable Energies, Faculty of New Science and Technologies, University of Tehran, Tehran, Iran

<sup>5</sup> CORIA-UMR 6614—Normandie University, CNRS University and INSA of Rouen, 76000 Rouen, France

## Introduction

Nanofluids have attracted the researchers' attention in the field of thermal engineering due to their ability in improvement of heat transfer [1–4]. Their ability in augmentation of heat transfer is attributed to some reasons such as increment in thermal conductivity (TC) in single phase and nucleation site increase in boiling heat transfer [5–7]. For instance, Ramezanizadeh et al. [8] added nickel nanoparticles into the working fluid of a thermosyphon and observed reduction in its thermal resistance. Improvement in the performance of the thermosyphon was mainly

attributed to the increment in both TC and nucleation sites. Similar conclusion was drawn by Nazari et al. [9] in the case of using graphene oxide nanofluid in a pulsating heat pipe. In addition to two-phase thermal mediums, nanofluids have shown the ability of heat transfer augmentation in single-phase devices [10–12]. For instance, Shirzad et al. [13] numerically investigated the performance of a pillow plate heat exchanger filled with various nanofluids and concluded that applying nanofluids can increase the heat transfer coefficient. In addition to the cooling appliances, nanofluids are used in different energy systems as shown in Fig. 1. Employing nanofluids in renewable energy technologies leads to higher energy extraction, size reduction and reliability improvement [14–16].

TC, specific heat and dynamic viscosity are among the factors with noticeable impact on the heat transfer ability of the fluids [23, 24]. Due to the importance of TC in the enhancement of heat transfer, it is crucial to distinguish the factors influencing this property. According to the literature review, size and concentration of solid particles, temperature and the type of base fluid are among the most important factors [25–27]. In addition to the mentioned ones, method of preparation, shape of the solid structures and the pH of the nanofluids affect their thermophysical and rheological features [25]. Generally, temperature and concentration increment results in improved TC. Moreover, nanofluids with the more conductive base fluids have higher TC. In the majority of previous researches conducted in the TC modeling of nanofluids, concentration and temperature have been used as inputs [28]. In some recent studies, size of particles is added as another variable to achieve more comprehensive regression [29, 30]. According to the study performed by Ahmadi et al. [31], although using the temperature and concentration as the inputs leads

to acceptable forecasting in some cases, considering the size of particles leads to the increase in the accuracy of the proposed model.

Different mathematical approaches are used in order to forecast and model the properties of nanofluids [32, 33]. Artificial intelligence is a powerful tool for various goals such as optimization and modeling the complex systems [34–37]. Intelligence models are applicable for predicting the dependent values by using appropriate inputs with perfect precision [38–41]. These models are useful for wide variety of applications such as predicting the thermal performance of heat exchangers and energy systems [10, 42, 43], energy consumption prediction [44], carbon dioxide emission [45], weather forecasting [44], etc. In addition, these approaches are able to forecast nanofluids' TC and dynamic viscosity with acceptable precision [33, 46, 47]. Ahmadi et al. [48] employed LSSVM-GA method to estimate the TC of  $\text{Al}_2\text{O}_3/\text{EG}$  nanofluid. The forecasted values by the proposed model were very close to the measured TCs, and the  $R$ -squared was 0.9902. In addition to the SVM-based methods, artificial neural networks (ANNs) are appropriate tools for prediction of nanofluids' TC. In a study [29], TC ratio of  $\text{CuO}/\text{EG}$  was predicted by utilizing GMDH and LSSVM-GA. The  $R$ -squared values of the mentioned approaches were 0.994 and 0.991, respectively. In addition to the high accuracy of the GMDH approach in forecasting the behavior of complex system, it has some features such as no requirement for predefinition of numbers of layers, neurons in hidden layer and active neurons [49] which make it favorable for predictive models. In addition, GMDH networks do not suffer from the training data overfitting [50].

The majority of the models represented for estimating the TC are applicable for the nanofluids with a single type of base fluid [51]. Proposing a model with the ability of forecasting the TC for various base fluids would be very useful for the researchers. In the current article, GMDH ANN, as an efficient algorithm, and a mathematical correlation, as an easy-to-use method, are employed to model the TC of nanofluids with dispersed  $\text{CuO}$  particles to provide applicable models. In addition, the confidence of the proposed models is compared on the basis of different statistical criteria to produce detailed insight into the employed forecasting models. The base fluids of the models nanofluids are water, ethylene glycol (EG) and engine oil. The inputs of the models are concentration and size of solid phase, TC of the base fluid and the temperature. All the data utilized for modeling are extracted from experimental studies.

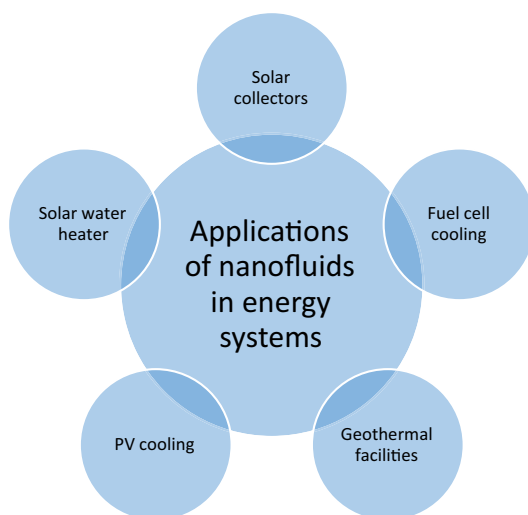


Fig. 1 Main applications of nanofluids in energy systems [14, 17–22]

### Methods

Mathematical correlations are employed to model the systems and features of the materials. These types of models have some advantages including simple structure and ease of utilization; however, due to their weakness in considering the interaction of variables affecting the outputs, they are not appropriate for complicated systems. ANNs are presented as intelligence approaches for modeling the systems with complex relationship between the inputs. In general, Voltera–Kolmogorov–Gabor (VKG) polynomials (Eq. 1) can be used in order to model complex systems containing set of data with multiple inputs and one output [52].

$$y = a_0 + \sum_{i=1}^n a_i x_i + \sum_{i=1}^n \sum_{j=1}^n a_{ij} x_i x_j + \sum_{i=1}^n \sum_{j=1}^n \sum_{k=1}^n a_{ijk} x_i x_j x_k + \dots \tag{1}$$

In Eq. 1,  $x = (x_1, x_2, \dots, x_n)$  are input vectors,  $y$  is model output, and  $a_i$  are coefficients of polynomial. VKG polynomials are approximated by second-order polynomials. These second-order polynomials are constructed based on the dual combinations of network inputs. GMDH algorithm is proposed based on this idea as the learning method for modeling complex systems [52, 53].

GMDH neural network has a structure of a multilayered and feed-forward network containing set of neurons created from linkage of different input pairs via second-order polynomial. Each layer in this network is established from one or more processing units that each of them has two inputs and one output. These units actually play the role of components constructing the model and are assumed as a second-order polynomial as given in Eq. 2 [52].

$$\hat{y}_n = a_0 + a_1 x_1 + a_2 x_2 + a_3 x_1 x_2 + a_4 x_1^2 + a_5 x_2^2 \tag{2}$$

Unknown parameters of GMDH algorithm are coefficients of the polynomial in Eq. 2. In order to calculate the output  $\hat{y}_i$  for each input vector  $x = (x_1, x_2, \dots, x_n)$  based on Eq. 2, the average of squared error (Eq. 3) must be minimized [54].

$$e = \sum_{i=1}^n (\hat{y}_i - y_i)^2 \tag{3}$$

To find the minimal of the error, partial derivative of Eq. 3 is used. By employing Eq. 2 in this partial derivative, a matrix equation ( $Aa = y$ ) is achieved. In this equation,  $a = \{a_0, a_1, a_2, a_3, a_4, a_5\}$ ,  $y = \{y_1, \dots, y_m\}^T$ , and matrix  $A$  is given in Eq. (4) [54].

$$A = \begin{bmatrix} 1 & x_{1p} & x_{1p} & x_{1p}^2 & x_{1p}^2 & x_{1p} & x_{1p} \\ 1 & x_{2p} & x_{2q} & x_{2p}^2 & x_{2q}^2 & x_{2p} & x_{2q} \\ 1 & x_{np} & x_{nq} & x_{np}^2 & x_{nq}^2 & x_{np} & x_{nq} \end{bmatrix} \tag{4}$$

One method to solve this matrix equation ( $Aa = y$ ) is using singular value decomposition (SVD) method. By using SVD method, the unknown coefficient  $a$  is calculated by Eq. 5 [52].

$$a = (A^T A)^{-1} A^T y \tag{5}$$

In Eq. 5,  $A^T$  is the transpose of the matrix  $A$ . With this method, unknown coefficient,  $a$ , can be calculated in most of the cases. If the matrix  $(A^T A)$  is non-invertible, Tikhonov method is applied to solve the equation.

In the design of GMDH neural network, the aim is to prevent the divergence of the network and relate shape and structure of the network to one or some numerical parameters in a way that by changing these parameters, the network structure changes as well. Evolution methods such as genetic algorithm have a vast application in different steps of designing the neural networks due to their unique capabilities in finding the optimum values and investigating the possibility in unpredictable spaces. In this paper, the genetic algorithm is used to design the shape of the neural network and determine its coefficients [53]. In order to make the GMDH neural networks widely recognized, the constraint of using adjacent layer in constructing the next level must be excluded. This type of neural networks is called GS in which to build new levels all the previous layers (as well as the input layer) are used [52, 53].

The criteria used in the current study for the evaluation of the regressions are  $R$ -squared, relative deviation (RD), mean square error (MSE) and average absolute relative deviation (AARD) which are defined as [55, 56]:

$$R^2 = 1 - \frac{\sum_{i=1}^{i=n} (y_i^{\text{experimental}} - y_i^{\text{predicted}})^2}{\sum_{i=1}^{i=n} (y_i^{\text{experimental}} - y^{\text{experimental}})^2}$$

$$RD_i = \frac{y_i^{\text{experimental}} - y_i^{\text{predicted}}}{y_i^{\text{experimental}}} \times 100$$

$$MSE = \frac{1}{n} \sum_{i=1}^{i=n} (y_i^{\text{experimental}} - y_i^{\text{predicted}})^2$$

$$AARD = \frac{1}{n} \sum_{i=1}^{i=n} \left| \frac{y_i^{\text{experimental}} - y_i^{\text{predicted}}}{y_i^{\text{experimental}}} \times 100 \right|$$

where  $y_i^{\text{experimental}}$  and  $y_i^{\text{predicted}}$  refer to the values of the data obtained in experimental studies and determined by the model, respectively.

## Results and discussion

Since the performance of a model in forecasting the output significantly depends on the input data, the variables used as inputs must be carefully defined. The majority of the researches carried out to model the TC of nanofluids have focused on a single type of nanofluid [57]. In these types of studies, the temperature and volume fraction of solid phase have been used as the inputs due to the noticeable dependency of TC on them [58, 59]. As shown in Fig. 2, increment in both of these factors leads to TC enhancement. Another factor considered in the recent studies, in order to reach more favorable precision and comprehensiveness, is the dimension of particles suspended in the base fluid. In addition, since the present models are designed to be

applicable for different nanofluids, the TC of the base fluids must be considered as another input. Generally, for the same concentration, temperature and size of particles, the nanofluids would have higher TC in the cases where the particles are suspended in more conductive fluids (as shown in Fig. 3).

In the present research, the data are extracted from several experimental studies. The ranges of the inputs and the base fluids are given in Table 1. The base fluids of the investigated nanofluids are ethylene glycol (EG), water and engine oil. In order to consider the impact of the base fluids' TC on the outputs of the model, their values for each fluids at 20 °C are used as one of the inputs. Moreover, temperature, volume fraction and the size of solid phase are the other inputs. In the first step, a model is proposed by

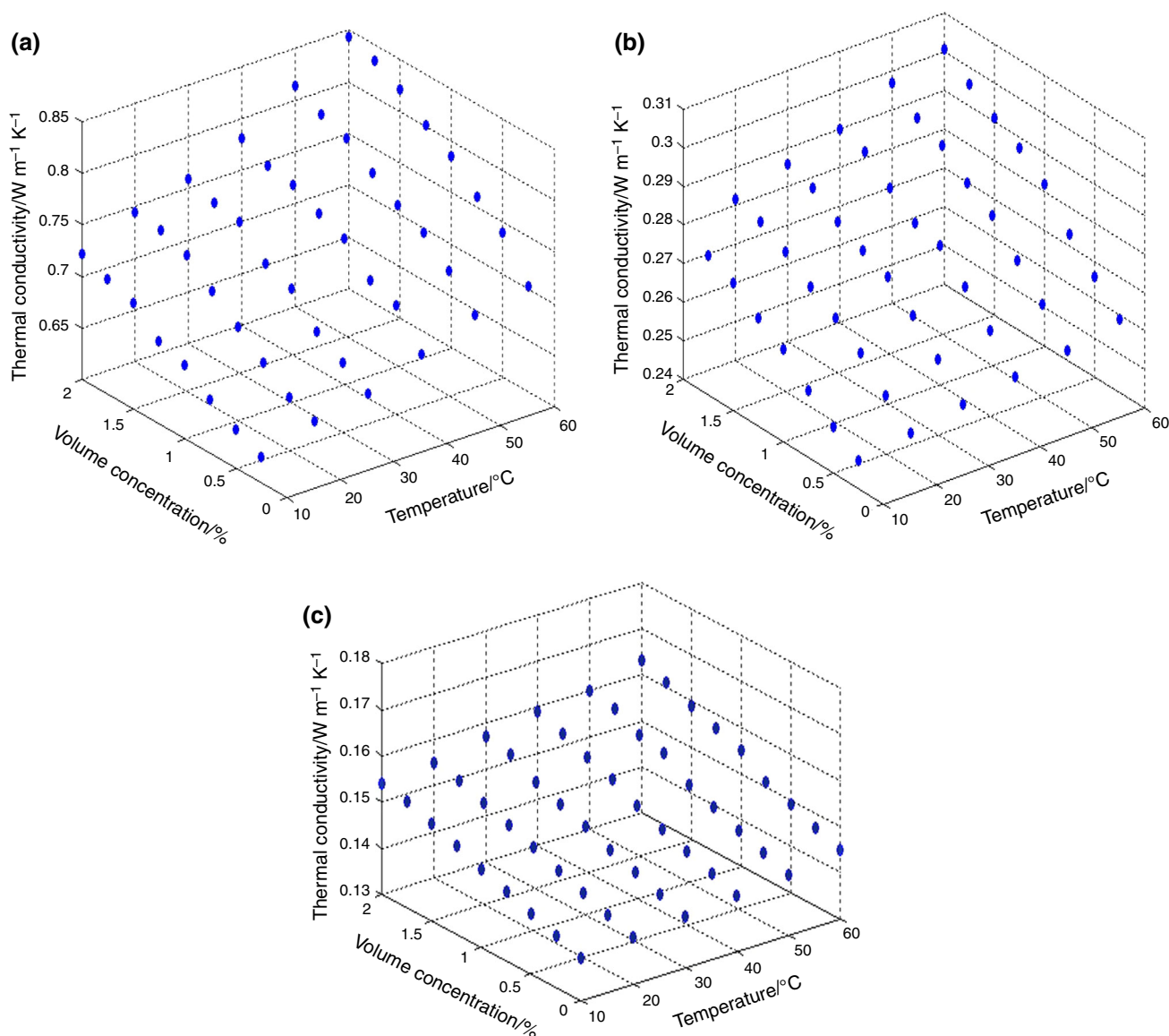


**Fig. 2** Effects of concentration and temperature on the TC of **a** CuO/water, **b** CuO/EG, and **c** CuO/engine oil nanofluids [60]

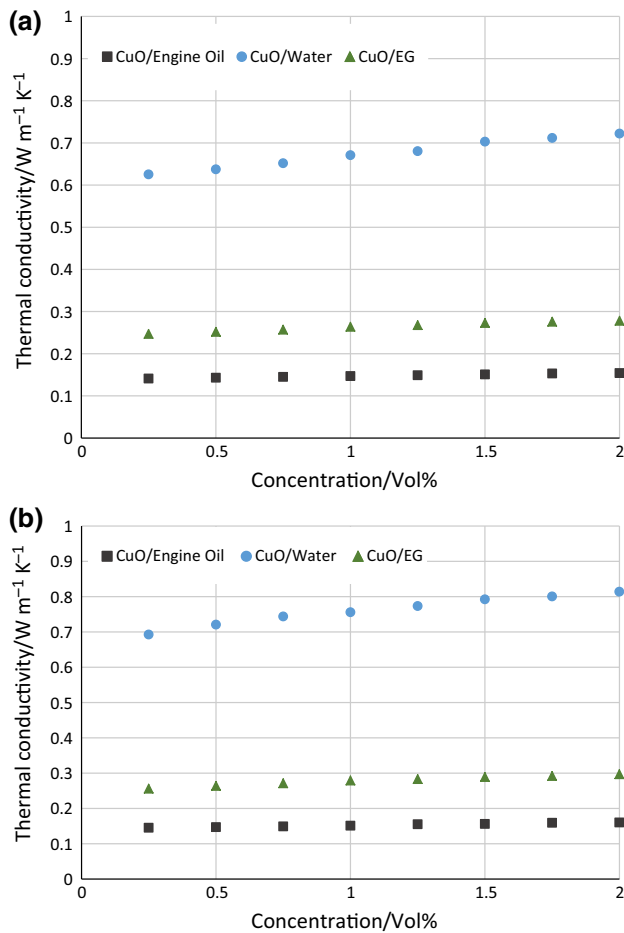


Fig. 3 TC of the nanofluids with various base fluids. a 10 °C, b 50 °C

Table 1 The variation ranges of the inputs [60–67]

Inputs	Range
Base fluids	Engine oil, water and ethylene glycol
Temperature/°C	10–70
Volumetric concentration/%	0–14.725
Size/nm	18.6–55

applying a polynomial. The structure of polynomial is shown in Eq. 6.

$$\begin{aligned}
 TC = & A * x_1 + B * x_2 + C * x_3 + D * x_4 + E * x_1^2 \\
 & + F * x_2^2 + G * x_3^2 + H * x_4^2 + I * x_1 * x_2 + J * x_1 x_3 \\
 & + K * x_1 * x_4 + L * x_2 * x_3 + M * x_2 * x_4 \\
 & + N * x_3 * x_4 + O
 \end{aligned}
 \tag{6}$$

where  $x_1, x_2, x_3$  and  $x_4$  are temperature, volume fraction, size and the TC of the base fluids, respectively. In this equation, the value of  $O$ , as the constant of the proposed

model, is equal to 0.31859. The obtained coefficients of the abovementioned correlations are given in Table 2.

One of the conventional criteria used for the assessment of regression is  $R$ -squared value. The closeness of this value to 1 means high accuracy of the model. In Fig. 4, the  $R$ -squared of the polynomial regression is represented by comparing the outputs and the measured TC in the experimental studies. As shown in Fig. 4, the value of the  $R$ -squared in the case where polynomial is utilized is equal to 0.9862. The majority of the predicted TC values are located in the vicinity of the actual data, which means acceptable accuracy of the regression.

In order to gain deeper insight, the relative deviation (RD) of the regression for each data is shown in Fig. 5. As it can be observed, the maximum absolute RD (ARD) is approximately 22.5%; however, most of the data are well predicted and their ARD is lower than 5%. The high value of the maximum ARD can be due to the weakness of the proposed polynomial regression in considering the complex interactions of the inputs. This problem can be solved by employing ANNs which have more advanced structure and are able to more accurate forecasting.

As indicated in the previous sections, the mathematical regression is not as accurate as the ANNs in modeling the systems. In this regard, GMDH shell software is applied for modeling the TC of the nanofluids with various base fluids based on GMDH ANN approach. The obtained relationships between the inputs and the TC of the considered nanofluids are given in “Appendix”. In Fig. 6, the data are compared to determine the  $R$ -squared. In this case, the  $R$ -squared is equal to 0.9996. Comparing the  $R$ -squared determined in the cases where polynomial regression and GMDH are employed reveals the higher accuracy of the regression by using the ANN.

Similar to the regression obtained by the polynomial, the values of RD are determined for each data index in the case of employing GMDH ANN for the regression, as shown in Fig. 7. The outputs are closer to the actual data when the GMDH ANN is used in comparison with the polynomial. More favorable precision of the model by using the ANN can be due to its more complex structure, which leads to better consideration of inputs interaction. In this case, the maximum ARD is approximately 6.3% which is much lower than the similar value when the polynomial regression is used. Moreover, the RD for the majority of the data is in the bound of  $\pm 2\%$ . These values of RD reveal the reliability and appropriate precision of the GMDH in forecasting the TC values of the nanofluids with CuO nanoparticles.

In order to assess the overall performance of the proposed regressions in modeling the TC of the nanofluids, average absolute relative deviation (AARD) values of the models are compared. As shown in Fig. 8, AARD values



**Table 2** Coefficients of the correlation

$A = 0.012691$	$B = -0.01054$	$C = 0.008593$	$D = 0.728172$	$E = 1.75 \times 10^{-6}$	$F = -0.00035$	$G = 4.7 \times 10^{-5}$
$H = 0.13926$	$I = 0.00045$	$J = -0.00025$	$K = 0.004144$	$L = 0.000441$	$M = -0.00029$	$N = 0.002965$

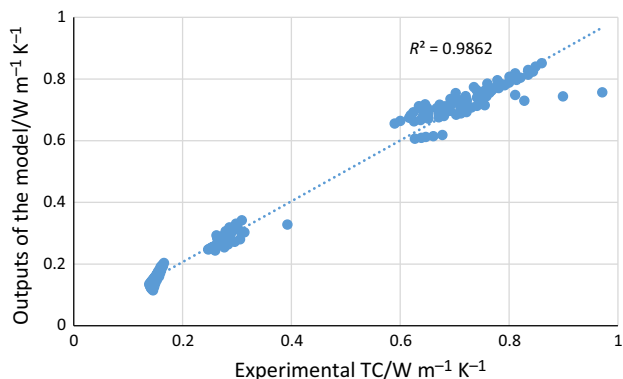


**Fig. 4** Comparison of the TC values by using polynomial regression

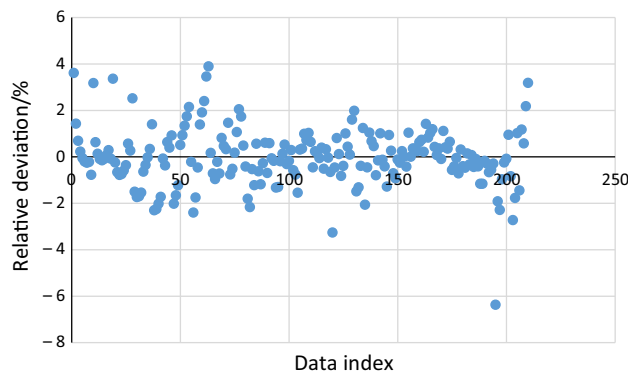


**Fig. 7** Relative deviation of the regression by using the GMDH ANN

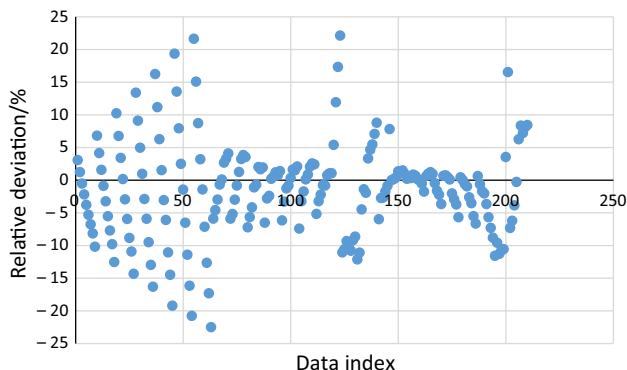


**Fig. 5** Relative deviation of the regression by using the polynomial

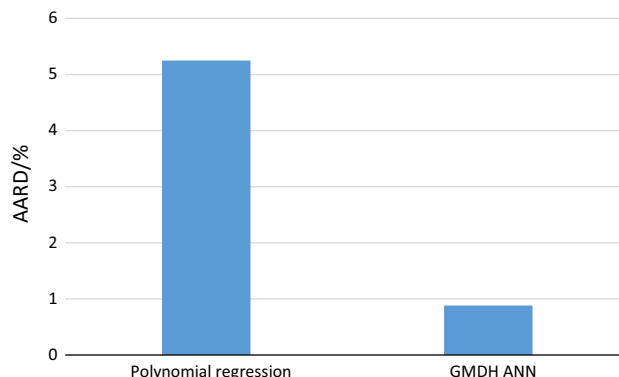


**Fig. 8** Comparison of AARD values for the correlation and ANN regressions

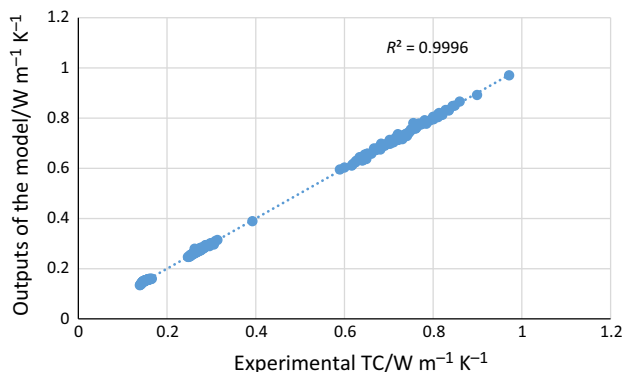


**Fig. 6** Comparison of the TC values by GMDH ANN

for the correlation and the ANN are approximately 5.25% and 0.881%, respectively. These values reveal much more perfection of the GMDH ANN in forecasting the TC of the nanofluids, which is similar to the results of the previous

studies focused on the other nanofluids. In addition to AARD, MSE values for both regressions are calculated to evaluate the models based on this criterion. The calculated MSE values in the cases where the mathematical correlation and GMDH ANN are employed are approximately  $9.28 \times 10^{-4}$  and  $2.36 \times 10^{-5}$ , respectively. According to all of the considered statistical criteria, it is demonstrated that applying the GMDH method results in more accurate regression compared with the correlation. This means that the predicted data by the ANN are closer to the values determined by the correlation as shown in Fig. 9. The accuracy of the ANN-based models is more obvious for the nanofluids with higher TC values.

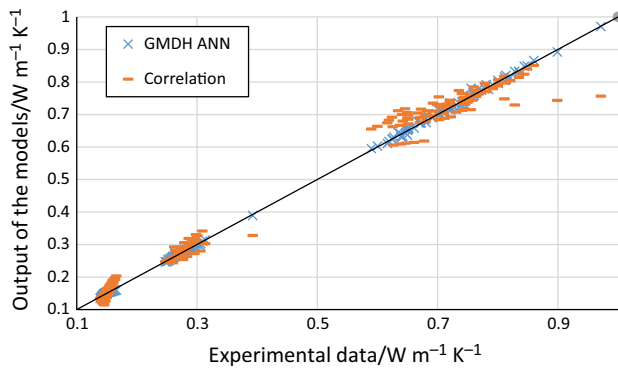


**Fig. 9** Comparison the data obtained by the models and actual values

## Conclusions

Due to the crucial role of nanofluids' thermal conductivity (TC) in their thermal behavior, it is important to propose models with reliable performance in predicting this thermophysical feature. In this article, the accuracies of group method of data handling (GMDH) artificial neural network (ANN) and a polynomial correlation in modeling the TC of nanofluids, containing CuO nanoparticles with three types of base fluids, were evaluated and compared. The employed inputs for the both models were temperature, TC of the base fluids, size and volume fraction of the nano-sized solid phase. According to the values of statistical criteria, including AARD and  $R$ -squared, employing GMDH ANN resulted in much more accuracy. The determined values of  $R$ -squared for the ANN and polynomial were 0.9996 and 0.9862, respectively. The values of AARD for the mentioned methods were approximately 0.881% and 5.25%, respectively.

## Appendix

$$\begin{aligned}
 N156 &= 0.0638187 + N250 * 2.30293 \\
 &+ N250 * N264 * 23.5634 - (N250)^2 * 13.7886 \\
 &- N264 * 1.68318 - (N264)^2 * 9.33539 \\
 N264 &= 0.0432462 + N377 * 0.0323191 \\
 &+ N377 * N315 * 0.403573 + N315 * 0.482274 \\
 &+ (N315)^2 * 0.363301 \\
 N315 &= -0.806049 + N345 * 0.801919 \\
 &+ N345 * N380 * 0.592981 - (N345)^2 * 0.0493165 \\
 &+ N380 * 3.74782 - (N380)^2 * 4.28298 \\
 N250 &= -0.00466728 - N335 * 0.446895 \\
 &- N335 * N357 * 27.6001 + (N335)^2 * 15.9285 \\
 &+ N357 * 1.43754 + (N357)^2 * 11.6728
 \end{aligned}$$

$$\begin{aligned}
 N323 &= 0.00163454 - N350 * 5.08638 \\
 &- N350 * N353 * 32.6077 + (N350)^2 * 32.5894 \\
 &+ N353 * 6.08958 \\
 N350 &= 0.293485 - \sqrt[3]{x_4} * 1.64301 + (\sqrt[3]{x_4})^2 * 2.37782 \\
 &+ N377 * 0.182398 \\
 N60 &= 0.0214562 - N197 * N77 * 4.09698 \\
 &+ (N197)^2 * 2.28313 + N77 * 0.854643 \\
 &+ (N77)^2 * 1.96742 \\
 N77 &= -0.0235764 - N332 * 0.243521 \\
 &- N332 * N185 * 54.0984 \\
 &+ (N332)^2 * 26.1746 + N185 * 1.40135 \\
 &+ (N185)^2 * 27.7079 \\
 N185 &= 0.000925156 + N266 * 0.717883 \\
 &+ N266 * N284 * 9.61885 \\
 &- (N266)^2 * 5.14743 + N284 * 0.272103 \\
 &- (N284)^2 * 4.43229 \\
 N284 &= 0.0131173 + \sqrt[3]{x_2} * 0.0105856 \\
 &+ \sqrt[3]{x_2} * N320 * 0.0680691 \\
 &+ N320 * 0.782995 + (N320)^2 * 0.140752 \\
 N320 &= -1.18285 + \sqrt[3]{x_3} * 0.809801 \\
 &+ \sqrt[3]{x_3} * N334 * 0.122827 \\
 &- (\sqrt[3]{x_3})^2 * 0.13057 + N334 * 0.458137 \\
 &+ (N334)^2 * 0.0931282 \\
 N266 &= 0.740175 - \sqrt[3]{x_4} * 4.94909 \\
 &- \sqrt[3]{x_4} * N335 * 14.4033 + (\sqrt[3]{x_4})^2 * 7.61967 \\
 &+ N335 * 6.04715 + (N335)^2 * 6.09104 \\
 N335 &= -0.878954 + N356 * 1.16337 \\
 &- N356 * N380 * 0.405506 \\
 &+ (N356)^2 * 0.0176024 + N380 * 3.83443 \\
 &- (N380)^2 * 4.01012 \\
 N197 &= -0.947113 + N380 * 4.34746 \\
 &+ N380 * N302 * 0.391864 \\
 &- (N380)^2 * 4.90199 + N302 * 0.896456 \\
 &- (N302)^2 * 0.0559059 \\
 N302 &= 0.00439602 - N339 * 1.49386 \\
 &- N339 * N357 * 67.8386 \\
 &+ (N339)^2 * 37.3589 + N357 * 2.47456 \\
 &+ (N357)^2 * 30.4492 \\
 N339 &= 0.00924584 + N345 * 0.716211 \\
 &+ N345 * N375 * 0.256732 \\
 &+ (N345)^2 * 0.179385 + N375 * 0.0486508 \\
 N129 &= -0.0617473 - N344 * N217 * 27.9366 \\
 &+ (N344)^2 * 13.1372 + N217 * 1.40366 \\
 &+ (N217)^2 * 14.3235
 \end{aligned}$$

$$\begin{aligned}
N217 &= 0.0372683 - N298 * 2.21564 \\
&\quad - N298 * N299 * 3.82076 \\
&\quad + (N298)^2 * 3.83466 + N299 * 2.97188 \\
&\quad + (N299)^2 * 0.242383 \\
N298 &= -0.00461328 - N338 * 0.605155 \\
&\quad - N338 * N357 * 37.0172 \\
&\quad + (N338)^2 * 20.7828 + N357 * 1.65003 + (N357)^2 * 16.1369 \\
N357 &= 0.224904 - \sqrt[3]{x_4} * 1.55475 - \sqrt[3]{x_4} * N375 * 0.51028 \\
&\quad + (\sqrt[3]{x_4})^2 * 2.47322 + N375 * 0.443408 \\
N375 &= -1.3152 + \sqrt[3]{x_2} * \sqrt[3]{x_3} * 0.0459091 \\
&\quad + \sqrt[3]{x_3} * 1.11126 - (\sqrt[3]{x_3})^2 * 0.186381 \\
N338 &= 0.0129124 + N345 * N356 * 43.7902 - (N345)^2 * 21.8442 \\
&\quad + N356 * 0.911248 - (N356)^2 * 21.7936 \\
N344 &= -0.477016 + N353 * 1.12265 - N353 * N379 * 0.265719 \\
&\quad + N379 * 2.10893 - (N379)^2 * 2.25038 \\
N353 &= -0.0220018 + N356 * 0.994495 + N377 * 0.0584774 \\
N48 &= -0.000454786 - N69 * N71 * 0.870543 \\
&\quad + (N69)^2 * 0.868246 + N71 * 1.00227 \\
N71 &= 0.0109597 - N139 * N214 * 50.1732 + (N139)^2 * 25.6696 \\
&\quad + N214 * 0.921561 + (N214)^2 * 24.5636 \\
N214 &= -0.0144738 + N331 * 1.08299 - N331 * N269 * 19.656 \\
&\quad + (N331)^2 * 7.87523 + (N269)^2 * 11.6828 \\
N269 &= -0.285722 + N380 * 1.126 - N380 * N303 * 0.586986 \\
&\quad - (N380)^2 * 1.0272 + N303 * 1.25418 \\
N303 &= 0.00379619 + \sqrt[3]{x_2} * 0.0252342 + \sqrt[3]{x_2} * N334 * 0.0472854 \\
&\quad + N334 * 0.771192 + (N334)^2 * 0.17568 \\
N69 &= -0.0119576 + N273 * 1.07403 - N273 * N139 * 29.6595 \\
&\quad + (N273)^2 * 13.7071 + (N139)^2 * 15.8416 \\
N139 &= 1.31772 - \sqrt[3]{x_4} * 7.24065 - \sqrt[3]{x_4} * N268 * 15.7399 \\
&\quad + (\sqrt[3]{x_4})^2 * 9.82624 + N268 * 6.84983 + (N268)^2 * 6.10165 \\
N268 &= -0.9162 + N380 * 4.16699 + N380 * N336 * 0.265379 \\
&\quad - (N380)^2 * 4.69022 + N336 * 0.98972 - (N336)^2 * 0.0976737 \\
N336 &= 0.0171419 + \sqrt[3]{x_2} * 0.0106666 + \sqrt[3]{x_2} * N345 * 0.0751379 \\
&\quad + N345 * 0.748366 + (N345)^2 * 0.170354 \\
N273 &= -0.0680299 + N380 * 0.191049 - N380 * N304 * 0.643235 \\
&\quad + N304 * 1.20139 + (N304)^2 * 0.0835203 \\
N304 &= -0.0193152 + N334 * 0.777182 + N334 * N377 * 0.252188 \\
&\quad + (N334)^2 * 0.109905 + N377 * 0.0983817 \\
N118 &= 0.0155467 - N136 * 0.337627 - N136 * N223 * 22.2581 \\
&\quad + (N136)^2 * 12.3103 + N223 * 1.23063 + (N223)^2 * 10.046 \\
N223 &= -0.0208803 - N286 * 2.33259 + N286 * N299 * 41.8394 \\
&\quad - (N286)^2 * 15.7271 + N299 * 3.48829 - (N299)^2 * 26.2913 \\
N299 &= -0.0212474 + N331 * 0.802107 + N331 * N376 * 0.275152 \\
&\quad + (N331)^2 * 0.0724277 + N376 * 0.0897678
\end{aligned}$$

$$\begin{aligned}
N331 &= -0.676945 + \sqrt[3]{x_4} * 2.13489 - (\sqrt[3]{x_4})^2 * 0.948832 \\
&\quad - N334 * 0.303469 + (N334)^2 * 0.92214 \\
N286 &= 0.0171763 + N332 * 0.675503 + N332 * N376 * 0.481898 \\
&\quad + (N332)^2 * 0.116863 + N376 * 0.0098905 \\
N376 &= 3.96757 * 10^{-14} + N377 * 1 \\
N332 &= -0.254285 + N334 * 1.1415 - N334 * N380 * 0.346046 \\
&\quad + N380 * 0.997576 - (N380)^2 * 0.884078 \\
N334 &= 0.665183 - \sqrt[3]{x_1} * 0.151091 + \sqrt[3]{x_1} * \sqrt[3]{x_4} * 0.212101 \\
&\quad + (\sqrt[3]{x_1})^2 * 0.00618198 - \sqrt[3]{x_4} * 1.99001 + (\sqrt[3]{x_4})^2 * 2.16703 \\
N136 &= 0.0109802 - N247 * 0.896005 - N247 * N346 * 19.3321 \\
&\quad + (N247)^2 * 11.8366 + N346 * 1.81279 + (N346)^2 * 7.56095 \\
N346 &= -0.483901 + N354 * 1.11989 - N354 * N379 * 0.267761 \\
&\quad + N379 * 2.11768 - (N379)^2 * 2.224 \\
N379 &= -8.47397 + \sqrt[3]{x_3} * 3.10228 - \sqrt[3]{x_3} * N380 * 2.08197 \\
&\quad - (\sqrt[3]{x_3})^2 * 0.336827 + N380 * 16.7518 - (N380)^2 * 9.85072 \\
N354 &= -1.37254 * 10^{-13} + N356 * 1 \\
N356 &= 0.325471 + \sqrt[3]{x_2} * 0.0275276 \\
&\quad - \sqrt[3]{x_4} * 1.60857 + (\sqrt[3]{x_4})^2 * 2.35855 \\
N247 &= -0.818308 + N380 * 3.6748 - (N380)^2 * 4.05446 \\
&\quad + N329 * 1.06662 - (N329)^2 * 0.060733 \\
N329 &= 0.0216857 + N345 * 0.60242 + N345 * N377 * 0.531008 \\
&\quad + (N345)^2 * 0.173633 + N377 * 0.0189504 \\
N377 &= 0.0244881 + \sqrt[3]{x_1} * 0.0503244 \\
&\quad - \sqrt[3]{x_1} * \sqrt[3]{x_2} * 0.0191276 + \sqrt[3]{x_2} * 0.274573 \\
N345 &= 1.09654 + \sqrt[3]{x_3} * \sqrt[3]{x_4} * 0.427947 - (\sqrt[3]{x_3})^2 * 0.0443035 \\
&\quad - \sqrt[3]{x_4} * 3.60702 + (\sqrt[3]{x_4})^2 * 2.68179 \\
N380 &= 0.967148 - \sqrt[3]{x_1} * 1.74116 + \sqrt[3]{x_1} * \sqrt[3]{x_3} * 0.435543 + \\
&\quad (\sqrt[3]{x_1})^2 * 0.0204996 + \sqrt[3]{x_3} * 1.57949 - (\sqrt[3]{x_3})^2 * 0.452209.
\end{aligned}$$

## References

1. Mahian O, Kianifar A, Heris SZ, Wen D, Sahin AZ, Wongwises S. Nanofluids effects on the evaporation rate in a solar still equipped with a heat exchanger. *Nano Energy*. 2017;36:134–55. <https://doi.org/10.1016/J.NANOEN.2017.04.025>.
2. Ramezanizadeh M, Alhuyi Nazari M, Ahmadi MH, Açıklalp E. Application of nanofluids in thermosyphons: a review. *J Mol Liq*. 2018;272:395–402. <https://doi.org/10.1016/J.MOLLIQ.2018.09.101>.
3. Mahian O, Kianifar A, Kleinstreuer C, Al-Nimr MA, Pop I, Sahin AZ, et al. A review of entropy generation in nanofluid flow. *Int J Heat Mass Transf*. 2013;65:514–32. <https://doi.org/10.1016/J.IJHEATMASTRANSFER.2013.06.010>.
4. Karimipour A, D'Orazio A, Shadloo MS. The effects of different nano particles of  $Al_2O_3$  and Ag on the MHD nano fluid flow and heat transfer in a microchannel including slip velocity and



- temperature jump. *Phys E Low-Dimens Syst Nanostruct.* 2017;86:146–53. <https://doi.org/10.1016/J.PHYSE.2016.10.015>.
5. Gandomkar A, Saidi MH, Shafii MB, Vandadi M, Kalan K. Visualization and comparative investigations of pulsating ferrofluid heat. *Appl Therm Eng.* 2017. <https://doi.org/10.1016/j.applthermaleng.2017.01.068>.
  6. Alhuyi Nazari M, Ahmadi MH, Ghasempour R, Shafii MB. How to improve the thermal performance of pulsating heat pipes: a review on working fluid. *Renew Sustain Energy Rev.* 2018;91:630–8. <https://doi.org/10.1016/j.rser.2018.04.042>.
  7. Safaei MR, Safdari Shadloo M, Goodarzi MS, Hadjadj A, Goshayeshi HR, Afrand M, et al. A survey on experimental and numerical studies of convection heat transfer of nanofluids inside closed conduits. *Adv Mech Eng.* 2016;8:1687814016673569. <https://doi.org/10.1177/1687814016673569>.
  8. Ramezanizadeh M, Alhuyi Nazari M, Ahmadi MH, Chau K. Experimental and numerical analysis of a nanofluidic thermosiphon heat exchanger. *Eng Appl Comput Fluid Mech.* 2019;13:40–7. <https://doi.org/10.1080/19942060.2018.1518272>.
  9. Nazari MA, Ghasempour R, Ahmadi MH, Heydarian G, Shafii MB. Experimental investigation of graphene oxide nanofluid on heat transfer enhancement of pulsating heat pipe. *Int Commun Heat Mass Transf.* 2018;91:90–4. <https://doi.org/10.1016/j.icheatmasstransfer.2017.12.006>.
  10. Baghban A, Kahani M, Nazari MA, Ahmadi MH, Yan W-M. Sensitivity analysis and application of machine learning methods to predict the heat transfer performance of CNT/water nanofluid flows through coils. *Int J Heat Mass Transf.* 2019;128:825–35. <https://doi.org/10.1016/J.IJHEATMASSTRANSFER.2018.09.041>.
  11. Hemmat Esfe M, Saedodin S, Mahian O, Wongwises S. Heat transfer characteristics and pressure drop of COOH-functionalized DWCNTs/water nanofluid in turbulent flow at low concentrations. *Int J Heat Mass Transf.* 2014;73:186–94. <https://doi.org/10.1016/J.IJHEATMASSTRANSFER.2014.01.069>.
  12. Safaei M, Ahmadi G, Goodarzi M, Safdari Shadloo M, Goshayeshi H, Dahari M, et al. Heat transfer and pressure drop in fully developed turbulent flows of graphene nanoplatelets–silver/water nanofluids. *Fluids.* 2016;1:20. <https://doi.org/10.3390/fluids1030020>.
  13. Shirzad M, Ajarostaghi SSM, Delavar MA, Sedighi K. Improve the thermal performance of the pillow plate heat exchanger by using nanofluid: numerical simulation. *Adv Powder Technol.* 2019;30:1356–65. <https://doi.org/10.1016/J.APT.2019.04.011>.
  14. Ramezanizadeh M, Alhuyi Nazari M, Hossein Ahmadi M, Chen L. A review on the approaches applied for cooling fuel cells. *Int J Heat Mass Transf.* 2019;139:517–25. <https://doi.org/10.1016/J.IJHEATMASSTRANSFER.2019.05.032>.
  15. Salavati Meibodi S, Kianifar A, Niazmand H, Mahian O, Wongwises S. Experimental investigation on the thermal efficiency and performance characteristics of a flat plate solar collector using SiO<sub>2</sub>/EG–water nanofluids. *Int Commun Heat Mass Transf.* 2015;65:71–5. <https://doi.org/10.1016/J.ICHEATMASSTRANSFER.2015.02.011>.
  16. Toghyani S, Afshari E, Baniasadi E, Shadloo MS. Energy and exergy analyses of a nanofluid based solar cooling and hydrogen production combined system. *Renew Energy.* 2019;141:1013–25. <https://doi.org/10.1016/J.RENENE.2019.04.073>.
  17. Ahmadi MH, Ramezanizadeh M, Nazari MA, Lorenzini G, Kumar R, Jilte R. Applications of nanofluids in geothermal: a review. *Math Model Eng Probl.* 2018;5:281–5. <https://doi.org/10.18280/mmep.050402>.
  18. Kasaeian A, Eshghi AT, Sameti M. A review on the applications of nanofluids in solar energy systems. *Renew Sustain Energy Rev.* 2015;43:584–98. <https://doi.org/10.1016/J.RSER.2014.11.020>.
  19. Natarajan E, Sathish R. Role of nanofluids in solar water heater. *Int J Adv Manuf Technol.* 2009. <https://doi.org/10.1007/s00170-008-1876-8>.
  20. Ebaid MSY, Ghrair AM, Al-Busoul M. Experimental investigation of cooling photovoltaic (PV) panels using (TiO<sub>2</sub>) nanofluid in water–polyethylene glycol mixture and (Al<sub>2</sub>O<sub>3</sub>) nanofluid in water–cetyltrimethylammonium bromide mixture. *Energy Convers Manag.* 2018;155:324–43. <https://doi.org/10.1016/J.ENCONMAN.2017.10.074>.
  21. Meibodi SS, Kianifar A, Mahian O, Wongwises S. Second law analysis of a nanofluid-based solar collector using experimental data. *J Therm Anal Calorim.* 2016;126:617–25. <https://doi.org/10.1007/s10973-016-5522-7>.
  22. Ehyaei MA, Ahmadi A, Assad MEH, Hachicha AA, Said Z. Energy, exergy and economic analyses for the selection of working fluid and metal oxide nanofluids in a parabolic trough collector. *Sol Energy.* 2019;187:175–84. <https://doi.org/10.1016/J.SOLENER.2019.05.046>.
  23. Said Z, Rahman SMA, El Haj Assad M, Alami AH. Heat transfer enhancement and life cycle analysis of a shell-and-tube heat exchanger using stable CuO/water nanofluid. *Sustain Energy Technol Assess.* 2019;31:306–17. <https://doi.org/10.1016/J.SETA.2018.12.020>.
  24. Said Z, El Haj Assad M, Hachicha AA, Bellos E, Abdelkareem MA, Alazaizeh DZ, et al. Enhancing the performance of automotive radiators using nanofluids. *Renew Sustain Energy Rev.* 2019;112:183–94. <https://doi.org/10.1016/J.RSER.2019.05.052>.
  25. Ahmadi MH, Mirlohi A, Alhuyi Nazari M, Ghasempour R. A review of thermal conductivity of various nanofluids. *J Mol Liq.* 2018. <https://doi.org/10.1016/j.molliq.2018.05.124>.
  26. Hemmat Esfe M, Saedodin S, Bahraei M, Toghraei D, Mahian O, Wongwises S. Thermal conductivity modeling of MgO/EG nanofluids using experimental data and artificial neural network. *J Therm Anal Calorim.* 2014;118:287–94. <https://doi.org/10.1007/s10973-014-4002-1>.
  27. Hemmat Esfe M, Saedodin S, Mahian O, Wongwises S. Thermal conductivity of Al<sub>2</sub>O<sub>3</sub>/water nanofluids. *J Therm Anal Calorim.* 2014;117:675–81. <https://doi.org/10.1007/s10973-014-3771-x>.
  28. Ramezanizadeh M, Alhuyi Nazari M, Ahmadi MH, Lorenzini G, Pop I. A review on the applications of intelligence methods in predicting thermal conductivity of nanofluids. *J Therm Anal Calorim.* 2019. <https://doi.org/10.1007/s10973-019-08154-3>.
  29. Ahmadi M-A, Ahmadi MH, Fahim Alavi M, Nazemzadegan MR, Ghasempour R, Shamshirband S. Determination of thermal conductivity ratio of CuO/ethylene glycol nanofluid by connectionist approach. *J Taiwan Inst Chem Eng.* 2018. <https://doi.org/10.1016/J.JTICE.2018.06.003>.
  30. Ahmadi MH, Alhuyi Nazari M, Ghasempour R, Madah H, Shafii MB, Ahmadi MA. Thermal conductivity ratio prediction of Al<sub>2</sub>O<sub>3</sub>/water nanofluid by applying connectionist methods. *Colloids Surf A Physicochem Eng Asp.* 2018. <https://doi.org/10.1016/j.colsurfa.2018.01.030>.
  31. Ahmadi MH, Hajizadeh F, Rahimzadeh M, Shafii MB, Chamkha AJ. Application GMDH artificial neural network for modeling of Al<sub>2</sub>O<sub>3</sub>/water and Al<sub>2</sub>O<sub>3</sub>/ethylene glycol thermal conductivity. *Int J Heat Technol.* 2018;36:773–82.
  32. Sepyani K, Afrand M, Hemmat Esfe M. An experimental evaluation of the effect of ZnO nanoparticles on the rheological behavior of engine oil. *J Mol Liq.* 2017;236:198–204. <https://doi.org/10.1016/J.MOLLIQ.2017.04.016>.
  33. Ahmadi Nadooshan A, Hemmat Esfe M, Afrand M. Evaluation of rheological behavior of 10W40 lubricant containing hybrid nanomaterial by measuring dynamic viscosity. *Phys E Low-Dimens Syst Nanostruct.* 2017;92:47–54. <https://doi.org/10.1016/J.PHYSE.2017.05.011>.

34. Zhang W, Maleki A, Rosen MA. A heuristic-based approach for optimizing a small independent solar and wind hybrid power scheme incorporating load forecasting. *J Clean Prod.* 2019. <https://doi.org/10.1016/J.JCLEPRO.2019.117920>.
35. Maleki A, Khajeh MG, Rosen MA. Two heuristic approaches for the optimization of grid-connected hybrid solar–hydrogen systems to supply residential thermal and electrical loads. *Sustain Cities Soc.* 2017;34:278–92. <https://doi.org/10.1016/J.SCS.2017.06.023>.
36. Maleki A, Hajinezhad A, Rosen MA. Modeling and optimal design of an off-grid hybrid system for electricity generation using various biodiesel fuels: a case study for Davarzan, Iran. *Biofuels.* 2016;7:699–712. <https://doi.org/10.1080/17597269.2016.1192443>.
37. Malekan M, Khosravi A, Goshayeshi HR, Assad MEH, Garcia Pabon JJ. Thermal resistance modeling of oscillating heat pipes for nanofluids by artificial intelligence approach. *J Heat Transf.* 2019. <https://doi.org/10.1115/1.4043569>.
38. Maleki A, Khajeh MG, Rosen MA. Weather forecasting for optimization of a hybrid solar-wind–powered reverse osmosis water desalination system using a novel optimizer approach. *Energy.* 2016;114:1120–34. <https://doi.org/10.1016/J.ENERGY.2016.06.134>.
39. Gholipour Khajeh M, Maleki A, Rosen MA, Ahmadi MH. Electricity price forecasting using neural networks with an improved iterative training algorithm. *Int J Ambient Energy.* 2018;39:147–58. <https://doi.org/10.1080/01430750.2016.1269674>.
40. Ahmadi Nadooshan A, Hemmat Esfe M, Afrand M. Prediction of rheological behavior of SiO<sub>2</sub>-MWCNTs/10W40 hybrid nanolubricant by designing neural network. *J Therm Anal Calorim.* 2018;131:2741–8. <https://doi.org/10.1007/s10973-017-6688-3>.
41. Pakatchian MR, Saeidi H, Ziamolki A. CFD-based blade shape optimization of MGT-70(3)axial flow compressor. *Int J Numer Methods Heat Fluid Flow.* 2019. <https://doi.org/10.1108/HFF-10-2018-0603>.
42. Ahmadi MH, Tatar A, Alhuyi Nazari M, Ghasempour R, Chamkha AJ, Yan W-M. Applicability of connectionist methods to predict thermal resistance of pulsating heat pipes with ethanol by using neural networks. *Int J Heat Mass Transf.* 2018. <https://doi.org/10.1016/j.ijheatmasstransfer.2018.06.085>.
43. Ahmadi MH, Sadeghzadeh M, Raffiee AH, Chau K. Applying GMDH neural network to estimate the thermal resistance and thermal conductivity of pulsating heat pipes. *Eng Appl Comput Fluid Mech.* 2019;13:327–36. <https://doi.org/10.1080/19942060.2019.1582109>.
44. Zhang W, Maleki A, Rosen MA, Liu J. Sizing a stand-alone solar-wind-hydrogen energy system using weather forecasting and a hybrid search optimization algorithm. *Energy Convers Manag.* 2019;180:609–21. <https://doi.org/10.1016/J.ENCONMAN.2018.08.102>.
45. Rezaei MH, Sadeghzadeh M, Alhuyi Nazari M, Ahmadi MH, Astarai FR. Applying GMDH artificial neural network in modeling CO<sub>2</sub> emissions in four nordic countries. *Int J Low-Carbon Technol.* 2018;13:266–71. <https://doi.org/10.1093/ijlct/cty026>.
46. Mohamadian F, Eftekhar L, Haghghi Bardineh Y. Applying GMDH artificial neural network to predict dynamic viscosity of an antimicrobial nanofluid. *Nanomed J.* 2018;5:217–21. <https://doi.org/10.22038/NMJ.2018.05.00005>.
47. Hemmat Esfe M, Bahiraei M, Hajmohammad MH, Afrand M. Rheological characteristics of MgO/oil nanolubricants: experimental study and neural network modeling. *Int Commun Heat Mass Transf.* 2017;86:245–52. <https://doi.org/10.1016/J.ICHEATMASSTRANSFER.2017.05.017>.
48. Ahmadi MH, Ahmadi MA, Nazari MA, Mahian O, Ghasempour R. A proposed model to predict thermal conductivity ratio of Al<sub>2</sub>O<sub>3</sub>/EG nanofluid by applying least squares support vector machine (LSSVM) and genetic algorithm as a connectionist approach. *J Therm Anal Calorim.* 2019;135:271–81. <https://doi.org/10.1007/s10973-018-7035-z>.
49. Zendejboudi A, Saidur R, Mahbubul IM, Hosseini SH. Data-driven methods for estimating the effective thermal conductivity of nanofluids: a comprehensive review. *Int J Heat Mass Transf.* 2019;131:1211–31. <https://doi.org/10.1016/J.IJHEATMASSTRANSFER.2018.11.053>.
50. Pham DT, Liu X. Modelling and prediction using GMDH networks of Adalines with nonlinear preprocessors. *Int J Syst Sci.* 1994;25:1743–59. <https://doi.org/10.1080/00207729408949310>.
51. Ramezanizadeh M, Alhuyi Nazari M. Modeling thermal conductivity of Ag/water nanofluid by applying a mathematical correlation and artificial neural network. *Int J Low-Carbon Technol.* 2019. <https://doi.org/10.1093/ijlct/ctz030>.
52. Zoqi M, Ghamgosar M, Ganji M, Fallahi S. Application of GMDH and genetic algorithm in fraction in biogas from landfill modeling. *J Environ Sci Technol.* 2016;18:1–12.
53. Ahmadi MH, Ahmadi MA, Mehrpooya M, Rosen MA. Using GMDH neural networks to model the power and torque of a stirling engine. *Sustainability.* 2015;7:2243–55. <https://doi.org/10.3390/su7022243>.
54. Pourkiaei SM, Ahmadi MH, Hasheminejad SM. Modeling and experimental verification of a 25 W fabricated PEM fuel cell by parametric and GMDH-type neural network. *Mech Ind.* 2016;17:105. <https://doi.org/10.1051/meca/2015050>.
55. Ramezanizadeh M, Ahmadi MA, Ahmadi MH, Alhuyi Nazari M. Rigorous smart model for predicting dynamic viscosity of Al<sub>2</sub>O<sub>3</sub>/water nanofluid. *J Therm Anal Calorim.* 2018. <https://doi.org/10.1007/s10973-018-7916-1>.
56. Ramezanizadeh M, Ahmadi MH, Nazari MA, Sadeghzadeh M, Chen L. A review on the utilized machine learning approaches for modeling the dynamic viscosity of nanofluids. *Renew Sustain Energy Rev.* 2019;114:109345. <https://doi.org/10.1016/J.RSER.2019.109345>.
57. Hemmat Esfe M, Motahari K, Sanatizadeh E, Afrand M, Rostamian H, Reza Hassani Ahangar M. Estimation of thermal conductivity of CNTs-water in low temperature by artificial neural network and correlation. *Int Commun Heat Mass Transf.* 2016;76:376–81. <https://doi.org/10.1016/J.ICHEATMASSTRANSFER.2015.12.012>.
58. Adhami Dehkordi R, Hemmat Esfe M, Afrand M. Effects of functionalized single walled carbon nanotubes on thermal performance of antifreeze: an experimental study on thermal conductivity. *Appl Therm Eng.* 2017;120:358–66. <https://doi.org/10.1016/J.APPLTHERMALENG.2017.04.009>.
59. Asadi A, Asadi M, Rezaniakolaei A, Rosendahl LA, Afrand M, Wongwises S. Heat transfer efficiency of Al<sub>2</sub>O<sub>3</sub>-MWCNT/thermal oil hybrid nanofluid as a cooling fluid in thermal and energy management applications: an experimental and theoretical investigation. *Int J Heat Mass Transf.* 2018;117:474–86. <https://doi.org/10.1016/J.IJHEATMASSTRANSFER.2017.10.036>.
60. Agarwal R, Verma K, Agrawal NK, Duchaniya RK, Singh R. Synthesis, characterization, thermal conductivity and sensitivity of CuO nanofluids. *Appl Therm Eng.* 2016;102:1024–36. <https://doi.org/10.1016/j.applthermaleng.2016.04.051>.
61. Liu M-S, Lin MC-C, Huang I-T, Wang C-C. Enhancement of thermal conductivity with CuO for nanofluids. *Chem Eng Technol.* 2006;29:72–7. <https://doi.org/10.1002/ceat.200500184>.
62. Lee S, Choi SU-S, Li S, Eastman JA. Measuring thermal conductivity of fluids containing oxide nanoparticles. *J Heat Transf.* 1999;121:280. <https://doi.org/10.1115/1.2825978>.
63. Wang X, Xu X, Choi SU S. Thermal Conductivity of nanoparticle—fluid mixture. *J Thermophys Heat Transf.* 1999;13:474–80. <https://doi.org/10.2514/2.6486>.
64. Liu M, Lin M, Wang C. Enhancements of thermal conductivities with Cu, CuO, and carbon nanotube nanofluids and application of

- MWNT/water nanofluid on a water chiller system. *Nanoscale Res Lett.* 2011;6:297. <https://doi.org/10.1186/1556-276X-6-297>.
65. Das SK, Putra N, Thiesen P, Roetzel W. Temperature dependence of thermal conductivity enhancement for nanofluids. *J Heat Transfer.* 2003;125:567. <https://doi.org/10.1115/1.1571080>.
66. Mints HA, Roy G, Nguyen CT, Doucet D. New temperature dependent thermal conductivity data for water-based nanofluids. *Int J Therm Sci.* 2009;48:363–71. <https://doi.org/10.1016/j.iethermalsci.2008.03.009>.
67. Khedkar RS, Sonawane SS, Wasewar KL. Influence of CuO nanoparticles in enhancing the thermal conductivity of water and monoethylene glycol based nanofluids. *Int Commun Heat Mass Transf.* 2012;39:665–9. <https://doi.org/10.1016/j.icheatmasstransfer.2012.03.012>.

**Publisher's Note** Springer Nature remains neutral with regard to jurisdictional claims in published maps and institutional affiliations.